Journal of Electrostatics, 17 (1985) 193—208
Elsevier Science Publishers B.V., Amsterdam — Printed in The Netherlands

COMPARISON OF WIRE—PLATE AND PLATE—PLATE ELECTROSTATIC PRECIPITATORS IN LAMINAR FLOW

K.D. KIHM, M. MITCHNER and S.A. SELF

Mechanical Engineering Department, Stanford University, Stanford, California 94305 (U.S.A.)

(Received June 8, 1984; accepted in revised form January 5, 1985)

Summary

A comparison is made between wire—plate and plate—plate electrode systems used as collectors for two-stage precipitators in the case of laminar flow, for which the particle concentration distribution and the particle trajectories can be calculated by the method of characteristics. The comparison is first made on the basis that the applied field (applied voltage divided by the electrode spacing) is held the same for the two systems. In the plate—plate case the collection efficiency is a function only of the Deutsch parameter $De_0 \equiv (w_0/u)(L/d)$ and becomes 100% for $De_0 = 1$. In the wire—plate case the efficiency is lower and the Deutsch parameter required to attain 100% efficiency is an increasing function of (h/d), the ratio of the wire—wire spacing $(2h)$ to the duct width $(2d)$. This behavior reflects the fact that for equal applied voltages the space-averaged precipitating field is smaller for the wire—plate case, and implies that the precipitator must be made longer to achieve 100% efficiency. If however the comparison is made on the basis of equal space-average fields at the collector, it is found that the efficiency for the wire—plate case is essentially equal to that for the plate—plate case, independent of the wire—wire spacing.

Introduction

The transport of particles in a single-stage, wire-duct precipitator is extremely complex and still poorly understood for two principal reasons. First, the electric field, which controls both the charging of particles and their migration velocity, is a strong function of position. Second, to properly account for the contribution of diffusion to particle transport requires a knowledge of the turbulent flow field, which is strongly dependent on the duct geometry and the effects of corona wind.

The widely used Deutsch model [1], and more recently developed computer codes [2], ignore these complications by making two simplifying assumptions: (i) that the inhomogeneous electric field can be replaced by space-averaged values for calculating the particle charge and migration velocity; and (ii) that complete mixing (i.e. infinite turbulent diffusivity) prevails transverse to the gas flow direction, so that the particle concentration can be assumed uniform in each transverse plane. This model leads to

0304-3886/85/$03.30

the well-known Deutsch formula for the penetration P and collection efficiency η:

$$\eta = (1 - P) = 1 - \exp(-De) \tag{1}$$

Here, the Deutsch number $De \equiv (w/u)(L/d)$, where w is the particle migration velocity normal to the collector plate, u is the mean gas velocity, L is the precipitator length and d is the wire-to-plate spacing. It should be noted that generally w is an increasing function of particle size and that a Deutsch number $De \sim 6$ is required for an efficiency $\eta = 99.9\%$.

Often the Deutsch number is written as $De = w(A/\dot{V})$ where A is the collector plate area and $\dot{V}$ is the volumetric gas throughput, so that for a given value of w the specific collector area $(A/\dot{V})$ to attain a required efficiency can be calculated from eqn. (1). Moreover from efficiency measurements and a knowledge of A and $\dot{V}$, eqn. (1) is often used to determine an effective migration velocity w_{eff} which is found to depend on particle size as well as other parameters, and is used as a practical measure of performance.

To obtain a more correct and detailed understanding of particle transport in precipitators it is necessary to remove the two simplifying assumptions noted above, so as to take proper account of both the non-uniform field and finite particle diffusivity in the prevailing turbulent gas flow.

In recent work, Leonard et al. [3, 4] studied both theoretically and experimentally the effect of finite and uniform diffusivity D but retained, for simplicity, a uniform electric field. The efficiency was shown to depend not only on De but also on the electric Peclet number $Pe \equiv (wd/D)$, and to go over to the Deutsch limit for $Pe \to 0$, and to the laminar limit ($\eta = De$ for $De \leqslant 1$) as $Pe \to \infty$, corresponding to $D \to 0$.

In the present paper we examine for laminar flow ($D = 0$) the effect of taking account of the non-uniform electric field in a wire–plate collector stage of a two-stage precipitator with entering pre-charged particles. Specifically we compare the performance of a wire–plate collector with a plate–plate (uniform field) collector. In the absence of diffusion the problem is deterministic and one can solve the differential equation for the particle concentration distribution and the particle trajectories by the method of characteristics. The results reported here correspond to one limiting case of the more general and practical case of precipitation in the presence of both non-uniform fields and finite diffusivity, which problem is currently being investigated*.

Formulation

Consider a precipitator duct of width $2d$ with a uniform laminar flow of gas, velocity u, carrying a monodispersion of particles of radius a_p and charge q, as shown in Fig. 1. In assuming a uniform velocity u we neglect

*"Comparison of wire–plate and plate–plate electrostatic precipitators in turbulent flow", by K.D. Kihm, M. Mitchner and S.A. Self. Submitted to Journal of Electrostatics.

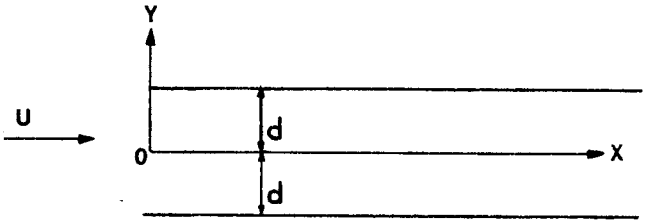

Fig. 1. Schematic of a duct precipitator. The planes $y = \pm d$ are the grounded collectors while the electrodes held at potential V_0 are disposed along the plane $y = 0$.

the effect of boundary layers and wakes from the electrodes. The planes $y = \pm d$ are the grounded collectors while the high voltage electrodes, having the same polarity as the particle charge, are disposed along the plane $y = 0$. Thus this model can represent either a parallel plate collector of width d, or half of a wire–plate precipitator of width $2d$ with the wires disposed along the center plane $y = 0$, so that in general the electric field is written $\vec{E} = \vec{E}(x,y)$.

The total particle velocity $\vec{w}$ can be written

$$\vec{w} = \hat{i}u + \vec{w}_E(x,y) \tag{2}$$

where $\vec{w}_E$ is the migration velocity relative to the gas and is given, neglecting inertia, by equating the Coulomb force to the Stokes' drag

$$\vec{w}_E(x,y) = \frac{q\vec{E}(x,y)}{6\pi a_p \eta_g} \equiv \mu \vec{E} \tag{3}$$

Here η_g is the gas viscosity and μ is the particle mobility.

The continuity equation for the particles of concentration $n(x,y)$ is

$$\nabla \cdot n\vec{w} \equiv n \nabla \cdot \vec{w} + \vec{w} \cdot \nabla n = 0 \tag{4}$$

Assuming that the aerosol is dilute and that there is no corona discharge, we may neglect space charge and assume that the field satisfies Laplace's equation $\nabla \cdot \vec{E} = 0$. Hence from eqns. (2) and (3) we have $\nabla \cdot \vec{w} = 0$, in which case eqn. (4) becomes

$$\vec{w} \cdot \nabla n = (u + w_{E_x}) \frac{\partial n}{\partial x} + w_{E_y} \frac{\partial n}{\partial y} = 0 \tag{5}$$

Further, by normalizing $\vec{E}$ on some characteristic field E_c, so that $\overline{E} \equiv E/E_c$, we may write eqn. (5) in the form

$$[u + w_c \overline{E}_x(x,y)] \frac{\partial n}{\partial x} + w_c \overline{E}_y(x,y) \frac{\partial n}{\partial y} = 0 \tag{6}$$

where

$$w_c \equiv \mu E_c \tag{6a}$$

is the migration velocity for the characteristic field E_c.

It is convenient to write eqn. (6) in the form

$$\frac{\partial n}{\partial x} + F(x,y)\frac{\partial n}{\partial y} = 0 \tag{7}$$

where

$$F(x,y) \equiv \frac{\epsilon_c \overline{E}_y(x,y)}{1 + \epsilon_c \overline{E}_x(x,y)} \tag{8}$$

and

$$\epsilon_c \equiv (w_c/u) \tag{8a}$$

For a homogeneous equation such as eqn. (7), the method of characteristics [5] yields the result that $n(x,y)$ is constant along the characteristic line given by:

$$\frac{dy}{dx} = F(x,y) \tag{9}$$

When inertia is neglected, as here, the characteristics are identical with the particle trajectories. Thus along a trajectory the concentration n remains constant at the value $n(0,y)$ set by the input boundary condition. That is to say, the input values of n propagate along the trajectories without change.

Since there is zero particle flux across the plane $y = 0$, it is clear that the x-directed flux across any downstream plane together with the y-directed flux integrated along the collector surface up to the same plane must add up to the input flux. Thus there are two alternative methods of calculating the penetration P and the efficiency $\eta = 1 - P$. For a uniform input concentration $n(0,y) = n_0$, the penetration is

$$P(x) = \frac{1}{n_0 u\, d}\int_0^d n(x,y)\, w_x(x,y)\, dy \tag{10}$$

while the collection efficiency is

$$\eta(x) = \frac{1}{n_0 u\, d}\int_0^x n(x',d)\, w_y(x',d)\, dx' \tag{11}$$

Solution for the plate–plate collector

In this simple case where, neglecting end effects at the entrance, we have a uniform field $\vec{E} = \hat{j}E_y = \hat{j}E_0 = \hat{j}(V_0/d)$, it is convenient to take the characteristic field $E_c = E_0$, so that $\vec{w}_E = \hat{j}w_0$, where $w_0 = \mu E_0$.

The equation for the trajectories takes the simple form

$$\frac{dy}{dx} = \epsilon_0 \tag{12}$$

where $\epsilon_0 \equiv (w_0/u)$.
Equation 12 integrates to

$$y = \epsilon_0 x + y_0 \tag{13}$$

Thus, as is intuitively obvious for this simple case, the trajectories are parallel straight lines inclined with slope (w_0/u) to the x-axis, as shown in Fig. 2.

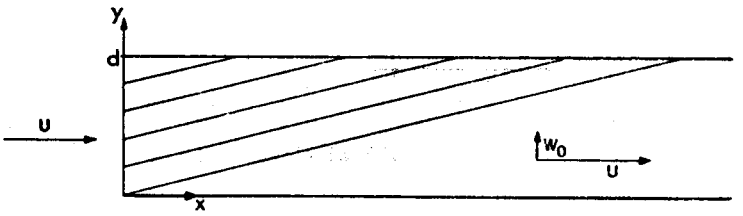

Fig. 2. Particle trajectories for the plate—plate case.

There is a limiting trajectory for $y_0 = 0$, which implies that all the particles entering at $x = 0$ are collected in a length $x = L = (d/\epsilon_0) = (ud/w_0)$, so that the efficiency becomes 100% for $De_0 = 1$.

The efficiency and penetration, calculated from either eqn. (10) or eqn. (11), is given by

$$\eta(x) \equiv 1 - P(x) = \frac{\epsilon_0 x}{d} = \frac{w_0 x}{u\,d} = De_0(x) \tag{14}$$

Thus the efficiency increases linearly with x, becoming 100% for $x = L = ud/w_0$, or $De_0 = 1$, as noted above.

Solution for a single wire—plate system

It is instructive to discuss the solution for a single wire—plate system before treating the multiple-wire case. Since the wire radius is normally very small compared with the half-width d, it is convenient to take the field as that given by a line charge of magnitude σ (C/m). Also, the origin of the x-coordinate is shifted so that the wire is located at $x = 0$ and the duct entrance is extended backwards to $x = -d$ as shown in Fig. 3.

The field for a line charge located midway between infinite parallel plates is given by [6]

$$E_x = \frac{\sigma}{4\epsilon_v d} \left\{ \frac{\sinh(\pi x/2d)\cos(\pi y/2d)}{\sinh^2(\pi x/2d) + \sin^2(\pi y/2d)} \right\} \tag{15a}$$

$$E_y = \frac{\sigma}{4\epsilon_v d}\left\{\frac{\cosh(\pi x/2d)\sin(\pi y/2d)}{\sinh^2(\pi x/2d)+\sin^2(\pi y/2d)}\right\} \tag{15b}$$

where ϵ_v is the vacuum permittivity.
In the following it is assumed that end effects are negligible, so that the field is given by eqns. (15) for $x > -d$ and is zero for $x < -d$.

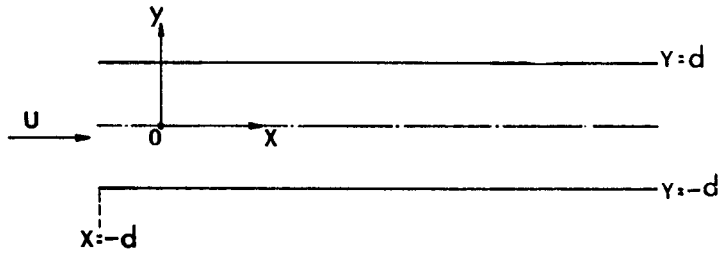

Fig. 3. Schematic of a single-wire-duct precipitator, with wire located at a distance d from the duct entrance.

It is convenient to take as the characteristic field the value of E_y at the plate surface directly opposite the wire, i.e.

$$E_c = E_y(0,d) = \sigma/4\epsilon_v d \tag{16}$$

Then

$$\epsilon_c \equiv \frac{w_c}{u} = \frac{\mu E_c}{u} = \frac{\mu}{u}\left(\frac{\sigma}{4\epsilon_v d}\right) \tag{17}$$

Using the normalized variables $\bar{x} = x/d$, $\bar{y} = y/d$, eqn. (9) for the particle trajectories becomes

$$\frac{d\bar{y}}{d\bar{x}} = \frac{\cosh(\pi\bar{x}/2)\sin(\pi\bar{y}/2)}{\frac{1}{\epsilon_c}\left[\sinh^2(\pi\bar{x}/2)+\sin^2(\pi y/2)\right]+\sinh(\pi\bar{x}/2)\cos(\pi\bar{y}/2)} \tag{18}$$

Numerical solutions of eqn. (18) have been obtained by Euler's method, for various initial values of $\bar{y}_0$ at the entrance plane $\bar{x} = -1$, as shown in Fig. 4 for a value of $\epsilon_c = 0.1$, a typical value for practical precipitators. It is seen that near the plane of the wire ($\bar{x} = 0$) the trajectories show a deflection

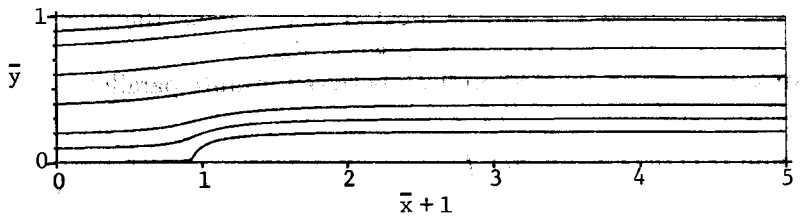

Fig. 4. Particle trajectories for a single-wire-duct precipitator; $\epsilon_c = 0.1$

towards the collector and that the deflection is most pronounced for particles passing closest to the wire.

There is a limiting trajectory for $y_0 = 0$ which has a bifurcation point upstream of the wire, where the characteristic line exhibits a $\pm$ 90° turn and continues either along the path indicated or its mirror image in the lower half plane. At the bifurcation point a particle is brought to rest as a result of an exact balance between the Coulomb force and the Stokes' drag of the passing gas. This occurs for $\sinh(\pi\bar{x}/2) = -\epsilon_c$, which for small ϵ_c gives the position as $\bar{x} \approx -2\epsilon_c/\pi$. In reality, particles will not accumulate at this point because the slightest perturbation, for instance due to Brownian motion, will cause them to be deflected and follow a path close to the limiting trajectory in the upper- or lower half plane.

The form of the characteristics $\bar{y}(\bar{x})$ close to the wire is discussed in the appendix, where it is shown that upstream of the wire there is an approximately circular region of radius (ϵ_c/π), centered at $\bar{x} = -(\epsilon_c/\pi)$, $\bar{y} = 0$, which particles entering the duct cannot penetrate because of the strong Coulomb repulsion near the wire.

Far downstream of the wire ($\bar{x} \gg 1$) the electric field becomes negligible and it is clear both intuitively and from eqn. (18) that the slope of the trajectories tends to zero i.e. they all become parallel to the x-axis. From numerical solutions for various values of ϵ_c, the location of the limiting trajectory $\bar{y}_L(\bar{x})$ has been determined as shown in Fig. 5. As is to be expected, the limiting trajectory is deflected more towards the collector as ϵ_c increases, and for $\epsilon_c > 0.5$ it intercepts the collector at a finite $\bar{x}$ position. The asymptotic value of $\bar{y}_L(\bar{x} \to \infty)$ is plotted as a function of ϵ_c for $\epsilon_c \leqslant 0.5$ in Fig. 6 from which it is seen that $\bar{y}_L\ (\bar{x} \to \infty) = 2\,\epsilon_c$ for $\epsilon_c \leqslant 0.5$.

For a uniform input concentration $n(0,y) = n_0$, the concentration profile is everywhere rectangular, having the value $n = n_0$ above the limiting trajectory and the value $n = 0$ below it. However the profile of the particle's axial velocity w_x, and hence of the axial flux $n_0 w_x$ is not in general rectangular. Only in the transverse plane of the wire and far downstream of the wire, where $E_x \to 0$, is the particle velocity profile rectangular at the value u. Upstream of the wire the profile is depressed below the value u, while downstream of the wire it is enhanced above the value u, because of the change of the sign in the E_x field component.

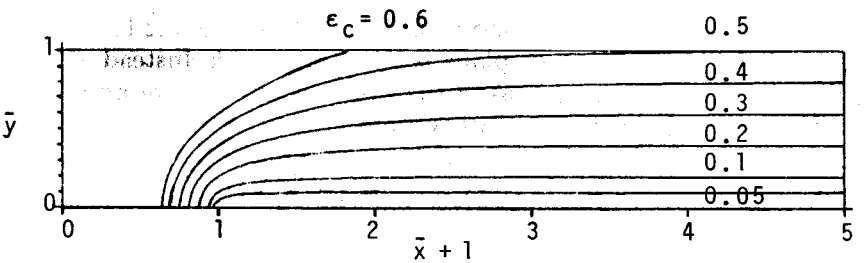

Fig. 5. Limiting trajectories for a single-wire-duct precipitator; for various values of ϵ_c.

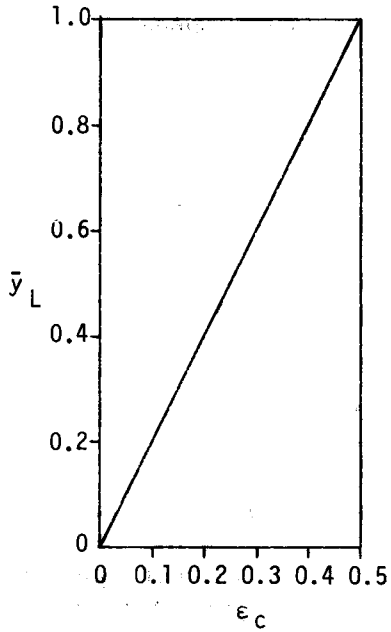

Fig. 6. Asymptotic deflection of limiting trajectory versus ϵ_c for a single-wire-duct system.

For $\epsilon_c \leqslant 0.5$ for which the limiting trajectory $\bar{y}_L$ becomes parallel to the axis for large $\bar{x}$, the collection efficiency can be calculated by noting that the particle flux is just $n_0 u(1 - \bar{y}_L(x \to \infty))$, so that the efficiency is $\eta = 2\epsilon_c$. For $\epsilon_c > 0.5$ when the limiting trajectory intercepts the collector, the efficiency becomes unity for a finite length which decreases as ϵ_c increases. However such large values of ϵ_c are not realizable in practice so that the attainment of 100% efficiency for a single wire—plate system is not of practical interest. On the other hand, as discussed below, a multiple wire—plate system can yeild 100% efficiency for arbitrarily small values of ϵ_c if it is made long enough.

Solution for multi-wire—plate system

The geometry considered here is shown in Fig. 7. The wires are located at $x = 0, 2h, 4h$ etc. and the entrance plane is taken at $x = -h$. Instead of representing the wires as line charges, as in the previous section, we now take account of the finite wire radius a. This is done so as to obtain a finite voltage V_0 and applied field $E_0 = V_0/d$, to allow a comparison to be made with the plate—plate case on the basis of equal applied fields.

For an infinite array of wires of radius a, and spacing $2h$ disposed symmetrically between infinite parallel plates of separation $2d$, the field components are given for $(a/d) \ll 1$, by:

$$E_x = E_0 \frac{\sum_{m=-\infty}^{\infty} \frac{\sinh[\pi(\bar{x} - 2m\bar{h})/2] \cos(\pi\bar{y}/2)}{\sinh^2[\pi(\bar{x} - 2m\bar{h})/2] + \sin^2(\pi\bar{y}/2)}}{\left(\frac{1}{\pi}\right) \sum_{m=-\infty}^{\infty} \ln \frac{\cosh(m\pi\bar{h}) + \cos(\pi\bar{a}/2)}{\cosh(m\pi\bar{h}) - \cos(\pi\bar{a}/2)}} \tag{19a}$$

$$E_y = E_0 \frac{\sum_{m=-\infty}^{\infty} \frac{\cosh[\pi(\bar{x} - 2m\bar{h})/2] \sin(\pi\bar{y}/2)}{\sinh^2[\pi(\bar{x} - 2m\bar{h})/2] + \sin^2(\pi\bar{y}/2)}}{\left(\frac{1}{\pi}\right) \sum_{m=-\infty}^{\infty} \ln \frac{\cosh(m\pi\bar{h}) + \cos(\pi\bar{a}/2)}{\cosh(m\pi\bar{h}) - \cos(\pi\bar{a}/2)}} \tag{19b}$$

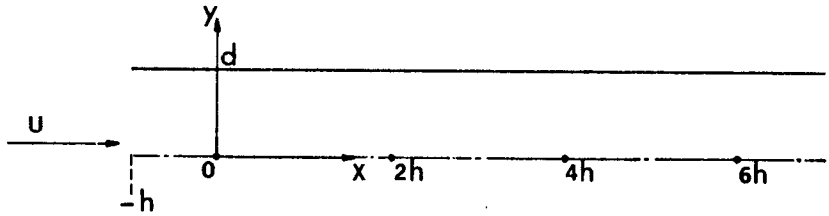

Fig. 7. Schematic for a multi-wire-duct precipitator.

Here, $E_0 = (V_0/d)$ is the applied field and $\bar{h} \equiv h/d$, $\bar{a} \equiv a/d$. For the semi-infinite system considered here, fringing field effects are neglected, so that the field is taken as zero for $x < -h$ and is given by eqns. (19) for $x > -h$. For $\bar{a} \ll 1$ and as $\bar{h} \to \bar{a}$, the fields given by eqns. (19) tend to the values $E_x \to 0$ and $E_y \to E_0$, so that the system tends to the parallel-plate case in this limit.

The equation for the characteristics or trajectories is given by eqn. (9) wherein $F(x,y)$ is given by eqn. (8) in which the field components are given by eqns. (19). Here, the characteristic field is taken as $E_c = E_0$, so that $w_c = w_0 = \mu E_0$ and $\epsilon_c = \epsilon_0 = w_0/u$.

The resulting equation has been numerically integrated for various values of ϵ_0, $\bar{h}$ and $\bar{a}$. The particle trajectories for the typical case $\epsilon_0 = 0.1$, $\bar{h} = 1$ and $\bar{a} = 0.01$ are shown in Fig. 8. It is seen that the limiting trajectory for a

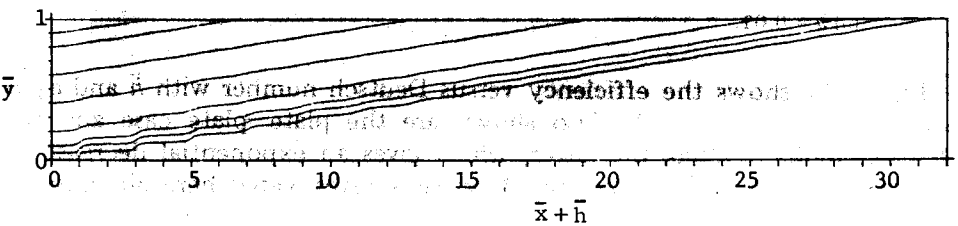

Fig. 8. Particle trajectories for a multi-wire-duct system for typical values $\epsilon_0 = 0.1$, $\bar{h} = 1$, $\bar{a} = 0.01$.

particle entering at ($\bar{x} = -\bar{h}$, $\bar{y}_0 = 0$) intercepts the collector at $\bar{x} \approx 30$ or, in terms of the distance from the duct entrance, $(\bar{x} + \bar{h}) = 31$. This corresponds to a Deutsch number of $De_0 = \epsilon_0 (\bar{x} + \bar{h}) \simeq 3.12$ for 100% efficiency.

Figure 9 shows the limiting trajectories for $\bar{h} = 1$ and $\bar{a} = 0.01$ for $\epsilon_0 = 0.1$, 0.2, 0.3. The duct lengths for 100% collection are $(\bar{x} + \bar{h}) = 31.2$, 15.7 and 10.6, so that the corresponding Deutsch numbers are $De_0 = 3.12$, 3.14, and 3.18. This indicates that the Deutsch number for 100% collection is a very weak function of ϵ_0 such that it increases slightly with ϵ_0. This comes about because as ϵ_0 increases, the number of wires effectively participating in the precipitation process decreases inversely, but the effects of the wires in producing deflections are not all equal.

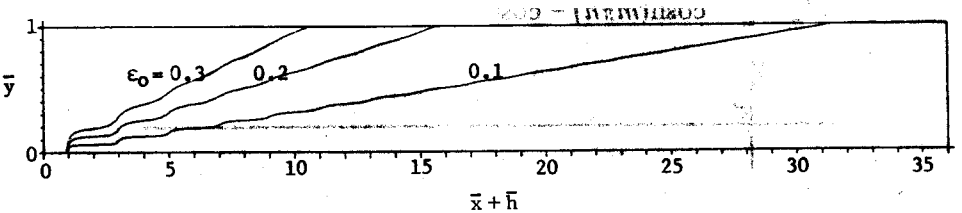

Fig. 9. Limiting trajectories for a multi-wire-duct system for $\bar{h} = 1$, $\bar{a} = 0.01$ and various values of ϵ_0.

In Fig. 10 are shown the limiting trajectories for $\epsilon_0 = 0.1$, $\bar{a} = 0.01$ and various values of $\bar{h}$. It is seen that for close-spaced wires, $\bar{h} = 0.1$, the limiting trajectory lies close to that for the plate—plate collector. As $\bar{h}$ increases, the limiting trajectories intercept the collector at increasing distances $(\bar{x} + \bar{h})$ from the duct entrance. Hence the Deutsch number for 100% collection increases with increasing $\bar{h}$.

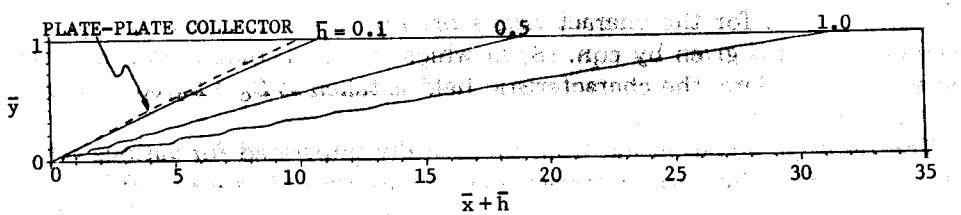

Fig. 10. Limiting trajectories for a multi-wire-duct system as a function of $\bar{h}$ for the case $\epsilon_0 = 0.1$ and $\bar{a} = 0.01$.

Figure 11 shows the efficiency versus Deutsch number with $\bar{h}$ and ϵ_0 as parameters for $\bar{a} = 0.01$. Also shown are the plate—plate case and the Deutsch model. Unlike the latter, which gives an exponential decrease of penetration with De, the laminar flow cases investigated here all show an asymptote where the efficiency becomes unity for a finite value of De_0. The Deutsch number for 100% efficiency is an increasing function of $\bar{h}$ such that it goes over to the plate—plate case as $\bar{h} \to 0$. The dependence of the efficiency on ϵ_0 is very weak for the cases considered.

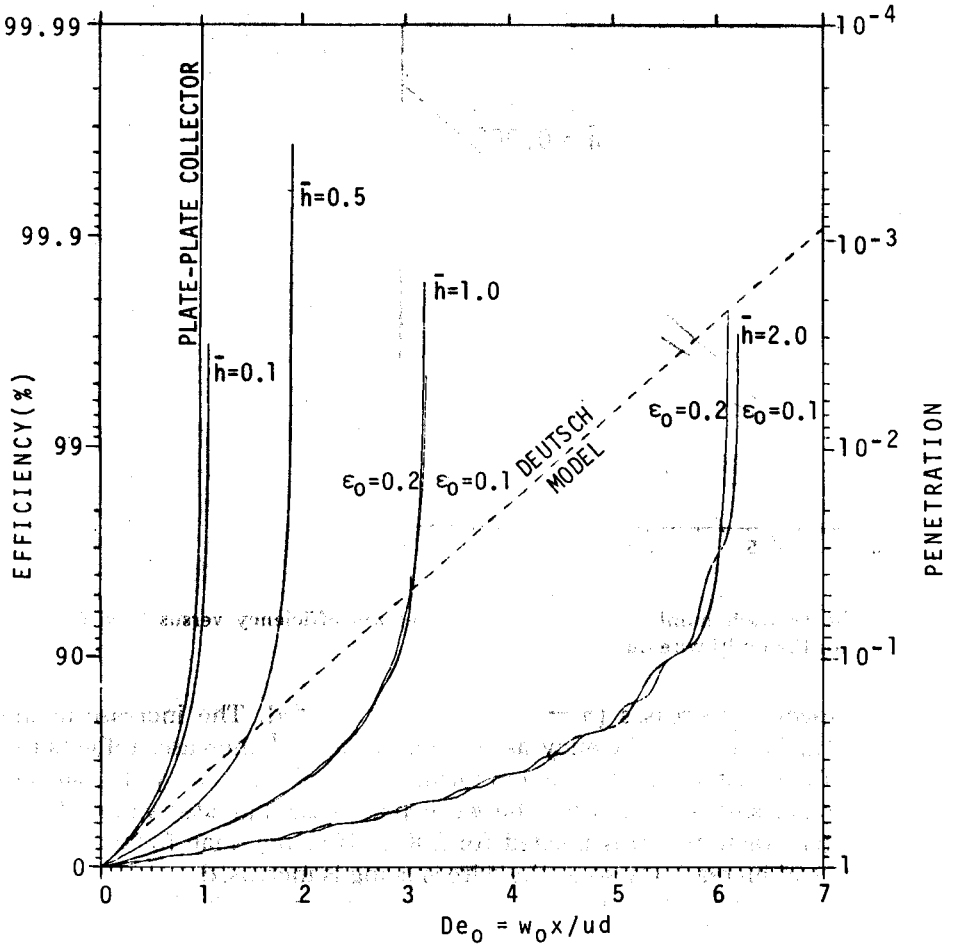

Fig. 11. Dependence of collection efficiency on Deutsch number for a multi-wire-duct system for $\epsilon_0 = 0.1, 0.2$, $\bar{h} = 0.1, 0.5, 1, 2$ and $\bar{a} = 0.01$. Also shown are the plate—plate and the Deutsch-model cases.

The dependence on wire diameter is shown in Fig. 12, where for $\epsilon_0 = 0.1$ the Deutsch number for 100% efficiency is plotted versus $\bar{h}$ with $\bar{a}$ as a parameter. For all $\bar{a}$ values the value of De_0 for 100% efficiency starts at unity for $\bar{h} = 0$ (the plate—plate limit) and tends to the straight line $De_0 \propto \bar{h}$ for $\bar{h} \gtrsim 1$. This behavior reflects the fact that for small $\bar{h}$, many wires contribute to the field at any given point, whereas for $\bar{h} \gtrsim 1$ the field opposite each wire is primarily due to that wire alone, with negligible contribution from adjacent wires.

In the foregoing treatment of the wire—plate collector, the Deutsch number De_0 was based on w_0, the migration velocity in the applied field $E_0 = V_0/d$. The fact that the Deutsch number De_0 for 100% efficiency for the wire—plate case goes over to the value $De_0 = 1$ for the plate—plate case as

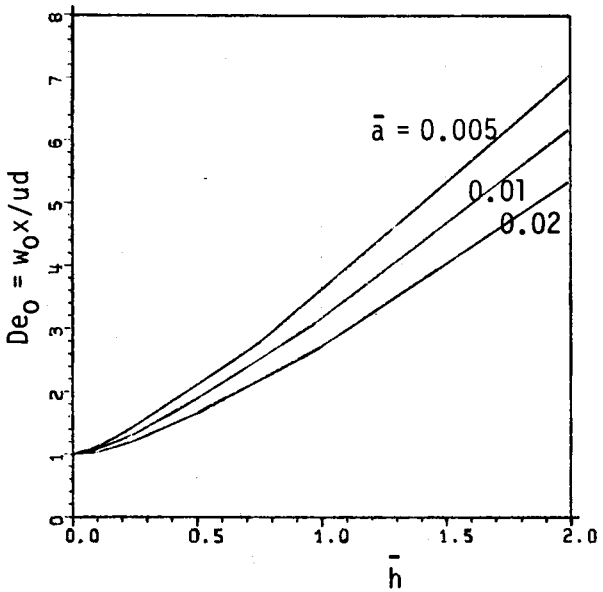

Fig. 12. The Deutsch number De_0 for 100% collection efficiency versus $\bar{h}$ with $\bar{a}$ as a parameter for the multi-wire-duct case with $\epsilon_0 = 0.1$.

the wire spacing decreases ($\bar{h} \to 0$) is to be expected. The increase in the value of De_0 for 100% efficiency as the wire spacing $\bar{h}$ increases reflects the fact that, for constant E_0, the precipitating field experienced by the particle is, on average, smaller. Thus for the wire—plate case a greater value of De_0 (i.e. a longer precipitator) is needed for 100% efficiency than for the plate—plate case, and increasingly so as the wire spacing is increased.

It may be argued that the foregoing comparison on the basis of equal values of applied field E_0 is less appropriate than a comparison based on equal values of some space-average field, in particular the space-average value at the collector surface $E_{av} \equiv \langle E_y(x,d) \rangle$. Figure 13 shows the ratio E_{av}/E_0, calculated from eqn. (19b), as a function of wire spacing $\bar{h}$, with the wire radius $\bar{a}$ as a parameter. As is to be expected, E_{av}/E_0 is a monotonically decreasing function of $\bar{h}$.

When the results of Fig. 11 are replotted against the average Deutsch number $De_{av} \equiv (w_{av}\bar{x}/u)$, based on $w_{av} \equiv \mu E_{av}$, as shown in Fig. 14, it is found that the efficiency curves for all values of $\bar{h}$ collapse on the curve for the plate—plate case. This useful result shows that the efficiency of a wire—plate precipitator is essentially the same as that of a plate—plate precipitator when they are compared on the basis of equal values of the space-average field at the collector. Of course, as the wire spacing is increased, the applied field $E_0 = (V_0/d)$ must be increased in order to maintain E_{av} at the same value.

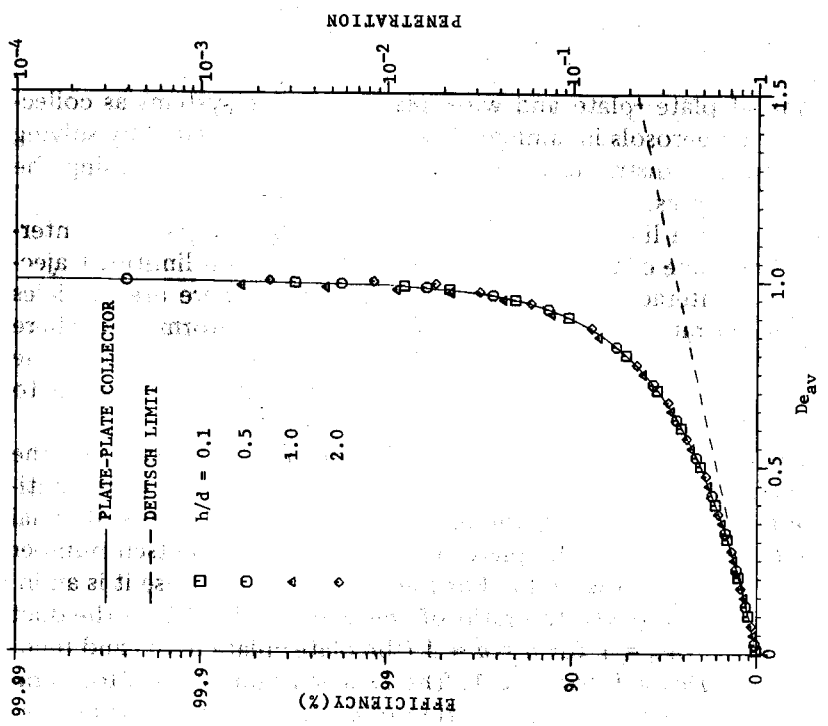

Fig. 14. Efficiency of wire-duct precipitators as a function of De_{av} for various wire—wire spacings.

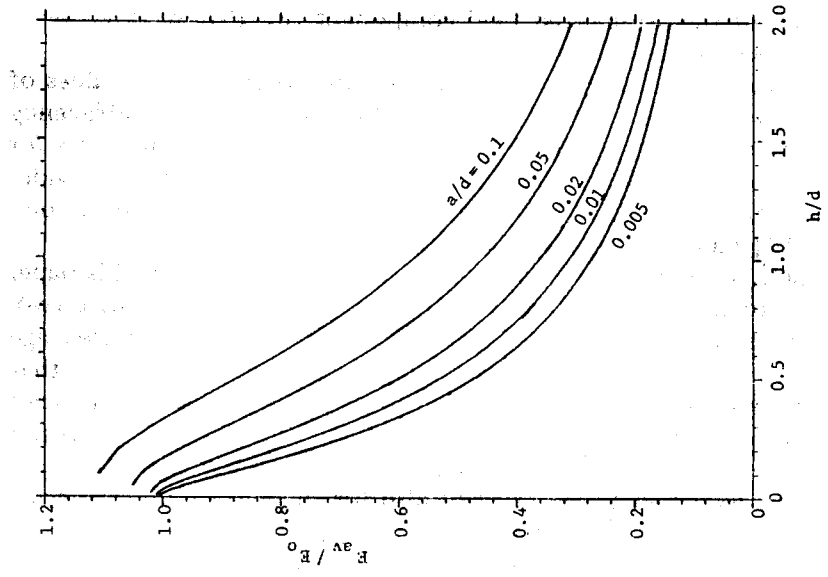

Fig. 13. Dependence of (E_{av}/E_o) on wire—wire spacing with wire radius as a parameter.

Conclusions

The behavior of plate—plate and wire—plate electrode systems as collectors for pre-charged aerosols in laminar flow has been investigated by solving for the concentration distribution and the particle trajectories using the method of characteristics.

In all cases there is a limiting trajectory, corresponding to particles entering the duct in the plane of the high-voltage electrode(s). This limiting trajectory separates the interaction space into regions where there are particles (of constant concentration if the input concentration is uniform) and where there are no particles. Moreover, where the limiting trajectory intercepts the grounded collector defines the length of the system which corresponds to 100% collection efficiency.

The Deutsch number for 100% efficiency, which is a measure of the precipitator length for complete collection, has been evaluated for the multi-wire-duct case and compared with the plate—plate case on the basis of equal applied fields $E_0 = V_0/d$. For the plate—plate system, the Deutsch number De_0 for complete collection is unity. For the multi-wire-duct case it is an increasing function of $\bar{h} \equiv (h/d)$, the ratio of the wire spacing $2h$ to the duct width $2d$, starting at $De_0 = 1$ for $\bar{h} = \bar{a} \ll 1$ (the plate—plate limit) and tending to straight lines $De_0 \propto \bar{h}$ for $\bar{h} \gtrsim 1$. The Deutsch number De_0 for complete collection is also a decreasing function of $\bar{a} = a/d$, the ratio of the wire diameter $(2a)$ to the duct width $(2d)$; it is also a weakly decreasing function of $\epsilon_0 \equiv (\mu E_0/u_0)$.

The ratio of the Deutsch number De_0 for complete collection for the multi-wire-duct case to that for the plate—plate case, is effectively an inverse measure of the field inhomogeneity in the former case. Physically, it is an inverse measure of the normalized field component (E_y/E_0), averaged along the limiting trajectory.

When, however, the comparison is made on the basis of equal values of the space-average field $E_{av} = \langle E_y(x,d) \rangle$, then it is found that the efficiency curves for all values of wire spacing $\bar{h}$ effectively collapse onto the curve for the plate—plate case and yield 100% efficiency for $De_{av} = 1$. This provides some justification for using E_{av} as the effective precipitating field in computer models [2] based on the Deutsch model.

In conclusion, it should be emphasized that the treatment in this paper applies strictly to the collection stage (without corona discharge) of a two-stage precipitator. It is not directly applicable to the case of a single-stage wire-duct precipitator where a corona discharge is present, because in that case the fields are considerably modified from those given by Laplace's equation as a result of ion space-charge. Nevertheless the results of this paper give insight into the effects of non-uniform fields on precipitator efficiency, which would be expected to be relevant also for single-stage precipitators.

Acknowledgements

This work was supported by the National Science Foundation under Grant No. CPE 8217719 and by the Electric Power Research Institute under Contract No. RP533-1.

References

1 H.J. White, Industrial Electrostatic Precipitation, Addison Wesley, 1963, Chap. 6.
2 J.R. McDonald, Computer simulation of the electrostatic precipitation process, Proceedings of International Conference on Electrostatic Precipitation, Monterey, California, October 1981, pp. 257—303.
3 G.L. Leonard, M. Mitchner and S.A. Self, Particle transport in electrostatic precipitators. Atmospheric Environment, 14 (1980) 1289—1299.
4 G.L. Leonard, M. Mitchner and S.A. Self, Experimental study of the effect of turbulent diffusion on precipitator efficiency. J. Aerosol Science 13 (1982) 271—284.
5 R. Courant and D. Hilbert, Methods of Mathematical Physics Vol. II. Interscience Publishers, 1962, Chap. 2.
6 M.R. Spiegel, Complex Variables (Schaum Series), McGraw-Hill, 1974, pp. 252—253.

Appendix

For the case of a single wire, represented as a line charge, between parallel ground plates, the behavior of the particle trajectories near the wire can be analyzed as follows.

The characteristics $y(x)$ are given by the solution of eqn. (18), i.e.

$$\frac{d\bar{y}}{d\bar{x}} = \frac{1}{\epsilon_c} \frac{\cosh(\pi\bar{x}/2)\sin(\pi\bar{y}/2)}{[\sinh^2(\pi\bar{x}/2) + \sin^2(\pi\bar{y}/2)] + \sinh(\pi\bar{x}/2)\cos(\pi\bar{y}/2)} \tag{A.1}$$

The locus of points where the characteristics have infinite slope is given by putting the denominator of (A.1) equal to zero, i.e.

$$[\sinh^2(\pi\bar{x}/2) + \sin^2(\pi\bar{y}/2)] + \epsilon_c \sinh(\pi\bar{x}/2)\cos(\pi\bar{y}/2) = 0 \tag{A.2}$$

For small ϵ_c it is evident that this locus occurs for small values of $\bar{x}$ and $\bar{y}$; hence, expanding the trigonometric and hyperbolic functions to second order in $\bar{x}$ and $\bar{y}$, gives the locus

$$\left(\bar{x} + \frac{\epsilon_c}{\pi}\right)^2 + \bar{y}^2 = \left(\frac{\epsilon_c}{\pi}\right)^2 \tag{A.3}$$

This is clearly a circle of radius (ϵ_c/π) centered at $(\bar{x} = -\epsilon_c/\pi,\ \bar{y} = 0)$, shown as the semi-circle in the upper half plane in Fig. 15. Outside this locus the slopes of the characteristics are always positive, while inside this locus the slopes of the characteristics are always negative.

The characteristics shown as solid lines in Fig. 15 were obtained by Euler's method, integrating downstream from the duct inlet at $\bar{x} = -1$. The

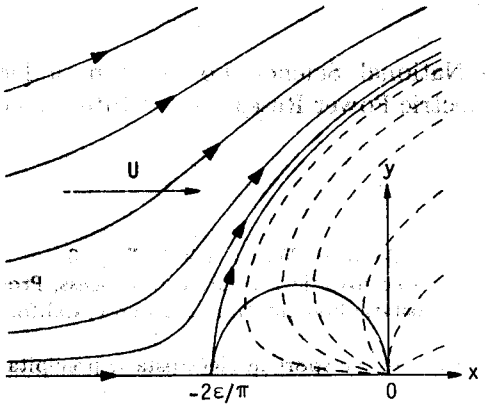

Fig. 15. The characteristics near the wire position for a single-wire-duct system.

broken lines show characteristics obtained by integrating back towards the wire for initial values of $\bar{y}$ lying below the limiting trajectory. These characteristics converge on the origin and those that intersect the locus (A.3) do so with infinite slope. Clearly these characteristics correspond to trajectories for particles released at the origin (i.e. the wire position) and, as such, are virtual trajectories of no physical interest to the problem in hand. No particles entering the duct at $\bar{x} = -1$ can penetrate the locus of infinite slope.

As is clear from Fig. 15, the limiting trajectory entering at $\bar{y} = 0$ has a bifurcation point at $\bar{x} = -(2\epsilon_c/\pi)$, where the particles come to rest, and then, after a deflection of $\pm \pi/2$, divides into two paths which are mirror images in the plane $\bar{y} = 0$.